Responses to Reviewer #2

Summary

This paper analyzes ground-based observations of traces gases acquired in an urban area of China during Fall 2018. The analysis focus is on oVOC observations and the contribution of oVOC to radical and ozone production. Using a box model, the study demonstrates that oVOC photolysis contributes significantly to primary radical production. The implication is that models that do not capture oVOC mixing ratios correctly (either due to missing emissions, inadequate chemical production, or other reasons) will have errors in calculation of ozone production rates and regimes. Publication is recommended following minor revisions.

Specific Comments

L118: Does this uncertainty influence the calculation of PROx from oVOC? If so, how much? I assume it is proportional to the PROx contributions of these unmeasured compounds. A simple way to calculate the error budget for this might be to take a root-sum-square of the uncertainties weighted by their PROx contributions for each species. This might provide some insight into which species we need to focus on for improved measurements/calibration. Just a suggestion.

Reply: Many thanks for your suggestions. We have included the discussion in the manuscript. We agree with the reviewer that the uncertainty of P(ROx) should be proportional to the P(ROx) contributions of these unmeasured compounds. By taking a root-sum-square of the uncertainties weighted by their P(ROx) contributions for each species, we found that the uncertainty of the concentrations of these species lead to uncertainty of 0.23 ppb h^{-1} in calculation of P(ROx), for the scenario of maximum OVOCs contribution to P(ROx). Given that the photolysis frequencies of carbonyls with large carbon numbers can vary several orders of magnitude, the uncertainty in photolysis frequencies is a more important factor that influence the calculation of P(ROx) from OVOCs than the uncertainty from measurement (only ~50%). To keep the smooth logic of the manuscript, we added this discussion about measurement uncertainty into supplement.

Line 47-59 in Supplement: The common OVOCs species were calibrated in this study. However, some OVOC species, including pyruvic acid, nitrophenol, methyl nitrophenol and carbonyls with large carbon number, were not calibrated. For these OVOC species, we used the method proposed by Sekimoto et al. (2017) to determine the relationship between VOC sensitivity and kinetic rate constants for proton transfer reactions of H_3O^+ with VOCs. The fitted line was used to determine the concentrations of those uncalibrated species. Following the discussions in Sekimoto, et al. (Sekimoto et al., 2017), the uncertainties of the concentrations for uncalibrated species were about 50 %. The uncertainties in the concentrations of these species lead to uncertainties of 0.04~0.23 ppb h-1 (1.3%~8.0%) in calculation of P(RO_X). Among these species, $C_nH_{2n-2}O_2$ (n>3) contributes the largest uncertainty, followed by $C_nH_{2n-4}O_2$ (n>3), $C_nH_{2n-4}O_3$ (n>3), $C_nH_{2n-2}O$ (n>3), $C_nH_{2n}O$ (n>5), pyruvic acid, nitrophenol and methyl nitrophenol.

L190: It is unnecessary to equate this to a deposition velocity. The 24h lifetime is a standard method in 0-D box modeling to account for all types of "physical loss," which might also include entrainment, advection, and other things. At least that's the hand-waving justification; the truth is that it is required to limit buildup of secondary species, because a 0-D model is an approximation of a 3-D atmosphere.
Reply: Thank you. We have deleted this sentence.

L191: Over what range were the sensitivity tests conducted?
Reply: We changed physical loss lifetime by 50% to test its effect on OH and HO_2 concentrations. A 50% change in physical loss lifetime leads to 3%, 6% and 10% changes in OH concentration, HO_2 concentration and P(O_3).

Line 205-207: A 50% change in the physical loss lifetime leads to 3%, 6% and 10%

changes in OH concentration, HO_2 concentration and ozone production rate.

L192: change “deposition” to “physical loss”.

Reply: Thank you. We have revised it.

Line 203-205: Sensitivity tests show that this assumed physical loss lifetime has a relatively small influence on the reactivity of modeled oxidation products, RO_X radicals and ozone production rates.

L255: Is this due to home heating, or from wild/agricultural fires?

Reply: We think it is more likely from wild/agricultural fires. Home heating is less likely as it was still warm in October and November in Guangzhou region. In addition, vehicle emission is another possible reason because the measurement site is close to heavy traffic.

Line 270-272: It is notable that acrolein, nitrophenol and methylnitrophenol all peaked at 20:00 in the evening, which is likely due to primary emissions e.g. biomass burning due to wild/agricultural fires (Ye et al., 2021) and vehicle emissions.

L259: Multiplying the y-axis values in Fig. S2 by k(OH+HCHO) or k(OH + pyruvic) might improve interpretation. Then, the scale is a unitless fractional contribution to OH reactivity. Also, it should be mentioned here and in the figure captions that each point is an average over one day of the campaign (I assume)

Reply: Thank you. We have revised it according to your suggestions. To distinguish the OH reactivity from reaction rate constant, we used R_{OH} rather than k_{OH} in the revised manuscript.

Line 82 in Supplement:

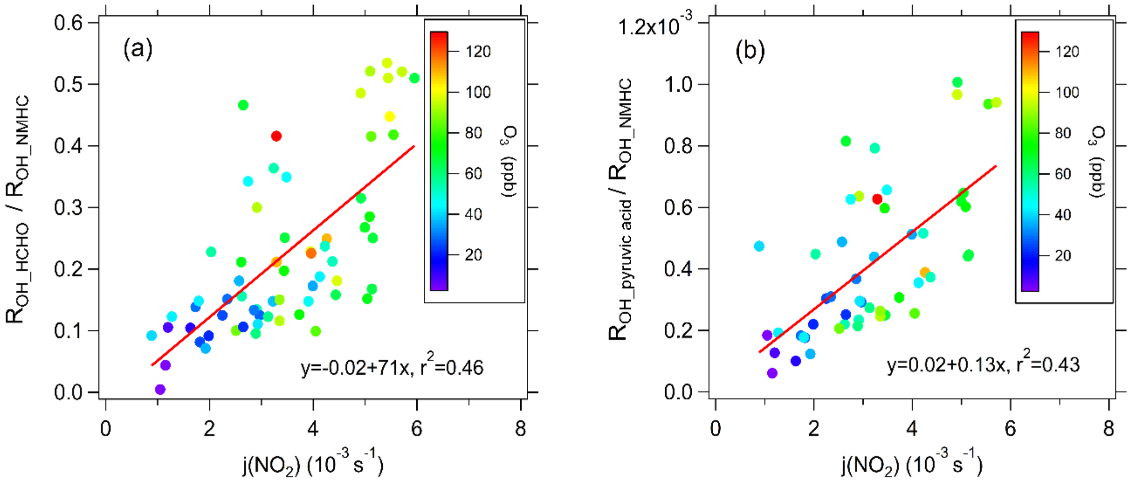

Figure S4. The scatter plot of daily daytime average R_{OH_HCHO} / R_{OH_NMHC} (and $R_{OH\_pyruvic\ acid}$ / R_{OH_NMHC}) ratios versus j(NO_2) color-coded using ozone concentrations during the campaign. Each point corresponds to a daytime average over one day of the campaign. Red lines are the linear fitting of the scatters.

L265: You mention the role of secondary pollution. Do the y-axis intercepts in Fig. S2 have any significance for contributions of primary emissions?

Reply: Yes, I think the y-axis intercepts can characterize contributions of primary emissions to some extent, because there is no secondary production at photolysis frequency value of zero. The intercepts for both R_{OH_HCHO} / R_{OH_NMHC} and $R_{OH\ pyruvic\ acid}$ / R_{OH_NMHC} are close to zero, indicating that primary emissions played a minor role in the concentration of two OVOCs.

L292 – 300: It would be more pertinent here to provide some quantitative metrics for how important oVOC was as a HOx source in these previous studies (either in ppb/h or %) to compare to the present analysis.

Reply: Many thanks. We have added this discussion in the manuscript.

Line 312-316: In total, OVOCs contributed 43% ~ 59% of P(ROX), which is higher than previous studies that reported OVOCs contributed 17%~40% of P(RO_X) in major cities in China and the US (Tan et al., 2019a;Tan et al., 2017;Tan et al., 2018;Tan et al., 2019b;Young et al., 2012;Griffith et al., 2016).

L348: How much does OH and HO2 increase between the case with oVOC constrained or not? It seems unlikely this would be a difference of 50% or more. Unless the oVOC contributions were even larger in those previous studies featuring HOx measurements?

Reply: Many thanks. We have added this discussion in the manuscript. The simulation of the box model without all observed OVOC species constrained underestimated $P(RO_X)$ by 16%~44% and underestimated OH and HO_2 by 15~38% and 25%~64% respectively, compared to the case with all observed OVOC species constrained.

Line 347-350: The underestimation of $P(RO_X)$ was 16% and 44% when using the lower and higher limits of OVOCs photolysis frequencies, respectively (red solid line and red dashed line in Figure 3a). In this case, the underestimation of OH and HO2 concentrations were 15~38% and 25%~64%, respectively.

L379: It would help less experienced readers to have some discussion/description on the conceptual definition of chain length.

Reply: Many thanks. ChL characterizes the number of iterations each RO_X radical makes prior to termination. It is equal to the ratio between the radical recycling rate and primary production rate, indicating the efficiency of radical propagation.

Line 413-416: ChL characterizes the number of iterations each RO_X radical makes prior to termination. It is equal to the ratio between the radical recycling rate and primary production rate (or equivalently, termination rate), indicating the efficiency of radical propagation.

L389: ChL for episode 1 is double the non-pollution value at mid-day (by eyeball).

Reply: Many thanks. Yes, ChL for episode 1 was a factor of 1.7 that in non-pollution period. We have modified this part.

Line 422-426: $P(O_3)$ in the two ozone pollution episodes was a factor of 2.6~2.8 that in the non-pollution period (Figure 5, Figure S8). $P(RO_X)$ in the two ozone

pollution episodes was a factor of 2.2~2.6 that in the non-pollution period. ChL in episode 2 was similar to that in non-pollution period, while ChL for episode 1 was a factor of 1.7 that in non-pollution period (Figure S8).

L396: This notion of radical amplification is also discussed in Qu et al. (2021), and that should probably be referenced here.

Reply: Many thanks. We have included this citation.

Line 433-434: These results indicate that the accelerating production of OVOCs had a significant positive feedback effect on ozone pollution (Qu et al., 2021).

L667: Is glyoxal included in the "others" block? Or is it not included here because it was not measured? I would expect glyoxal to be comparable to methylglyoxal as a ROx source. If this figure is limited to observed oVOC, this should be stated clearly in the caption and probably discussed in the text, since there are likely even more oVOC than those observed by the PTRMS.

Reply: Many thanks. This figure corresponds to the simulation result of box model with all observed OVOC species constrained. Therefore, the total P(RO$_X$) contains all observed OVOCs and simulated OVOCs that were not measured. The simulated OVOCs that were not measured was integrated into the "others" in Figure 2b, which includes glyoxal. Although the concentration of glyoxal (0.37 ppb) was slightly higher than that of methylglyoxal (0.32 ppb), the photolysis frequency of glyoxal (3.5*10^{-6} s^{-1}, daytime average) is far lower than that of methylglyoxal (5.5*10^{-5} s^{-1}, daytime average). As a result, P(RO$_X$) from glyoxal (0.010 ppb h^{-1}) is far lower than P(RO$_X$) from methylglyoxal (0.13 ppb h^{-1}). Note that Figure 2b shows the relative contributions of different non-HCHO OVOC species to P(RO$_X$) for the scenarios with minimum OVOC contribution to P(RO$_X$). We have added the scenario scenarios with maximum OVOC contribution to P(RO$_X$) in Supplement (Figure S5) of the revised manuscript.

Line 286-288: The simulated total P(RO$_X$) contains the contributions from all observed photodegradable species and several simulated OVOCs that was not

measured such as glyoxal.

Line 88 in Supplement:

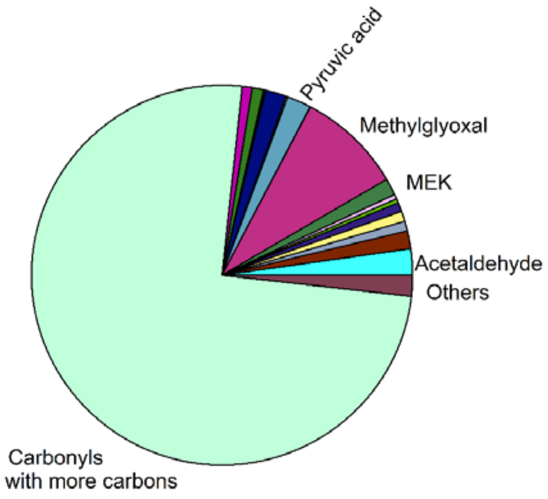

Figure S5. The relative contributions of non-HCHO OVOC species to P(RO$_X$) for the scenarios with maximum OVOC contribution to P(RO$_X$).

Lines 308-310: Figure 2b and Figure S5 show the relative contributions of different non-HCHO OVOC species to P(RO$_X$) for the scenarios with minimum and maximum OVOC contribution, respectively.

L687: Does the blue line use the "minimum" oVOCs contribution? If so, I think there should also be a dashed blue line for the maximum case, or just eliminate the dashed red line. As it stands, it is not clear what the blue line should be compared to.

Reply: The blue line represents the scenario without observed OVOCs constrained in the box model. For the scenario with observed OVOCs constrained (red lines), we cannot determine the contribution of carbonyls with more carbon number to P(RO$_X$) because they are not possible to assign into specific individual species. Therefore, using the possible ranges of photolysis frequencies of carbonyls with more carbon number, we can obtain the possible widest variation range of P(RO$_X$). The red solid line represents the minimum OVOCs contribution and the dashed red line represents the maximum OVOCs contribution. The blue line is lower than the red solid line and red dashed line, indicating the simulated P(RO$_X$) without observed OVOCs constrained is lower than that with observed OVOCs constrained for either minimum or maximum photolysis frequencies used.

Line 343-347: As shown in Figure 3a, the simulation of the box model without observed OVOC species constrained (blue line in Figure 3a) underestimated P(RO_X) significantly compared to the scenario with all observed OVOC species constrained (red lines in Figure 3a).

Line 386-389: As shown in Figure 3b, compared to the scenario with observed photodegradable OVOCs species constrained in box model (red lines in Figure 3b), the scenario without constraining observed OVOCs (blue line in Figure 3b) underestimated peak value of P(O_3) by 15~38%.

Technical Comments

L34: "comparable to"

Reply: Thank you. We have revised it.

L49: replace "hydroxide" with "hydrogen oxide"

Reply: Thank you. We have revised it.

L51: Recommend replacing "Photodegradable species…including" with "Photolysis of" and deleting "via photolysis reactions."

Reply: Thank you. We have revised it.

L139: PTR-ToF-MS

Reply: Thank you. We have revised it.

L202: "radicals"

Reply: Thank you. We have revised it.

L207: space after period

Reply: Thank you. We have revised it.

L270: delete “basically”

Reply: Thank you. We have revised it.

L271: “species and calculated photolysis frequencies derived from observed actinic flux.”

Reply: Thank you. We have deleted this sentence and added another one “The simulated total P(RO_X) contains the contributions from all observed photodegradable species and several simulated OVOCs that was not measured such as glyoxal.” to depict it more clearly.

L361: Start a new paragraph.

Reply: Thank you. We have revised it.

L424: Availability of model code?

Reply: Thank you. We have added it.

Line 462-463: The observational data and model code used in this study are available from corresponding authors upon request (byuan@jnu.edu.cn).

L543: Qu reference missing information.

Reply: Thank you. We have revised it.

L661: What is shading in Fig. 1?

Reply: Thank you. Lines and shading represent averages and standard deviations, respectively. We have explained it in the notation.

Lines 706-708: Figure 1. The average diurnal variations of the concentrations of photodegradable OVOCs species during the field campaign in Guangzhou. Lines and shading represent averages and standard deviations, respectively.

L667: ozonolysis is in this figure but never mentioned in the paper Supplement,

Reply: Many thanks. I have added a sentence to mention it.

Line 310-311: Ozonolysis of alkenes play a minor role in P(RO_X).

L57: Define ChL here.

Reply: Many thanks. I have defined ChL in lines 416-419 according to your suggestion.

Line 413-416: ChL characterizes the number of iterations each RO_X radical makes prior to termination. It is equal to the ratio between the radical recycling rate and primary production rate (or equivalently, termination rate), indicating the efficiency of radical propagation.

Table S1: 4th column is a mixing ratio, not concentration. Also you may wish to include measurement uncertainty here (your choice).

Reply: Thank you. We have modified it.

Lines 223-224: Table S1. Molecular formula, photolysis reactions, daytime average mixing ratio and photolysis frequencies of photodegradable species during the campaign.

References:

Burkholder, J., Sander, S., Abbatt, J., Barker, J., Cappa, C., Crounse, J., Dibble, T., Huie, R., Kolb, C., and Kurylo, M.: Chemical kinetics and photochemical data for use in atmospheric studies; evaluation number 19, Pasadena, CA: Jet Propulsion Laboratory, National Aeronautics and Space ⋯, 2020.

Griffith, S. M., Hansen, R., Dusanter, S., Michoud, V., Gilman, J., Kuster, W., Veres, P., Graus, M., de Gouw, J., and Roberts, J.: Measurements of hydroxyl and hydroperoxy radicals during CalNex-LA: Model comparisons and radical budgets, Journal of Geophysical Research: Atmospheres, 121, 4211-4232, 2016.

Jenkin, M. E., Saunders, S. M., and Pilling, M. J.: The tropospheric degradation of volatile organic compounds: a protocol for mechanism development, Atmos. Environ., 31, 81-104, 1997.

Qu, H., Wang, Y., Zhang, R., Liu, X., Huey, L. G., Sjostedt, S., Zeng, L., Lu, K., Wu, Y., and Shao, M.: Chemical Production of Oxygenated Volatile Organic Compounds Strongly Enhances Boundary-Layer Oxidation Chemistry and Ozone Production, Environmental Science & Technology, 55, 13718-13727, 2021.

Sekimoto, K., Li, S.-M., Yuan, B., Koss, A., Coggon, M., Warneke, C., and de Gouw, J.: Calculation of the sensitivity of proton-transfer-reaction mass spectrometry (PTR-MS) for organic trace gases using molecular properties, International Journal of Mass Spectrometry, 421, 71-94, 10.1016/j.ijms.2017.04.006, 2017.

Tan, Z., Fuchs, H., Lu, K., Hofzumahaus, A., Bohn, B., Broch, S., Dong, H., Gomm, S., Häseler, R., He, L., Holland, F., Li, X., Liu, Y., Lu, S., Rohrer, F., Shao, M., Wang, B., Wang, M., Wu, Y., Zeng, L., Zhang, Y., Wahner, A., and Zhang, Y.: Radical chemistry at a rural site (Wangdu) in the North China Plain: observation and model calculations of OH, HO2 and RO2 radicals, Atmos. Chem. Phys., 17, 663-690, 10.5194/acp-17-663-2017, 2017.

Tan, Z., Rohrer, F., Lu, K., Ma, X., Bohn, B., Broch, S., Dong, H., Fuchs, H., Gkatzelis, G. I., Hofzumahaus, A., Holland, F., Li, X., Liu, Y., Liu, Y., Novelli, A., Shao, M., Wang, H., Wu, Y., Zeng, L., Hu, M., Kiendler-Scharr, A., Wahner, A., and Zhang, Y.: Wintertime photochemistry in Beijing: observations of ROx radical concentrations in the North China Plain during the BEST-ONE campaign, Atmos. Chem. Phys., 18, 12391-12411, 10.5194/acp-18-12391-2018, 2018.

Tan, Z., Lu, K., Hofzumahaus, A., Fuchs, H., Bohn, B., Holland, F., Liu, Y., Rohrer, F., Shao, M., and Sun, K.: Experimental budgets of OH, HO 2, and RO 2 radicals and implications for ozone formation in the Pearl River Delta in China 2014, Atmospheric chemistry and physics, 19, 7129-7150, 2019a.

Tan, Z., Lu, K., Jiang, M., Su, R., Wang, H., Lou, S., Fu, Q., Zhai, C., Tan, Q., Yue, D., Chen, D., Wang, Z., Xie, S., Zeng, L., and Zhang, Y.: Daytime atmospheric oxidation capacity in four Chinese megacities during the photochemically polluted season: a case study based on box model simulation, Atmos. Chem. Phys., 19, 3493-3513, 10.5194/acp-19-3493-2019, 2019b.

Ye, C., Yuan, B., Lin, Y., Wang, Z., Hu, W., Li, T., Chen, W., Wu, C., Wang, C., Huang, S., Qi, J., Wang, B., Wang, C., Song, W., Wang, X., Zheng, E., Krechmer, J. E., Ye, P., Zhang, Z., Wang, X., Worsnop, D. R., and Shao, M.: Chemical characterization of oxygenated organic compounds in the gas phase and particle phase using iodide CIMS with FIGAERO in urban air, Atmospheric Chemistry and Physics, 21, 8455-8478, 10.5194/acp-21-8455-2021, 2021.

Young, C. J., Washenfelder, R. A., Roberts, J. M., Mielke, L. H., Osthoff, H. D., Tsai, C., Pikelnaya, O., Stutz, J., Veres, P. R., and Cochran, A. K.: Vertically resolved measurements of nighttime radical reservoirs in Los Angeles and their contribution to the urban radical budget, Environmental science & technology, 46, 10965-10973, 2012.